2019 IEEE 16th International Conference on Rehabilitation Robotics (ICORR)
Toronto, Canada, June 24-28, 2019

Improving the Accuracy of Wearable Sensors for Human Locomotion Tracking Using Phase-Locked Regression Models

Ton T. H. Duong, *Student Member, IEEE*, Huanghe Zhang, *Student Member, IEEE*,
T. Sean Lynch, Damiano Zanotto, *Member, IEEE*

***Abstract*— The trend toward soft wearable robotic systems creates a compelling need for new and reliable sensor systems that do not require a rigid mounting frame. Despite the growing use of inertial measurement units (IMUs) in motion tracking applications, sensor drift and IMU-to-segment misalignment still represent major problems in applications requiring high accuracy. This paper proposes a novel 2-step calibration method which takes advantage of the periodic nature of human locomotion to improve the accuracy of wearable inertial sensors in measuring lower-limb joint angles. Specifically, the method was applied to the determination of the hip joint angles during walking tasks. The accuracy and precision of the calibration method were accessed in a group of $N = 8$ subjects who walked with a custom-designed inertial motion capture system at 85% and 115% of their comfortable pace, using an optical motion capture system as reference. In light of its low computational complexity and good accuracy, the proposed approach shows promise for embedded applications, including closed-loop control of soft wearable robotic systems.**

***Index Terms*— wearable technology, inertial sensors, human motion analysis**

I. Introduction

Wearable robotics has become an increasingly popular research area in recent years. Exoskeletons, powered orthoses and robotic prostheses have shown great potential in both healthcare and military applications [1]–[5]. Despite recent advances in ergonomic designs, rigid-link exoskeletons are typically bulky and their kinematic structure may constrain the user's natural motions. Moreover, the mechanical impedance of the rigid links and any misalignment between the robot and the human joints can produce spurious interaction forces that cause discomfort [6], [7].

For these reasons, more recent design trends aim toward soft exoskeletons with artificial muscles or flexible actuators to maximize the device's transparency and reduce undesired interaction forces [2], [8]–[10]. As a result, traditional feedback sensors that require a rigid mounting frame (e.g., encoders, potentiometers, and load cells) have become unsuitable. The emerging soft exoskeletons, or exosuits, create a compelling need for new and reliable systems capable of sensing joint angles during walking and other highly-dynamic locomotion tasks, such as running and jumping. Available options include systems based on IMUs [11]–[13], conductive fibers [14], and hyperelastic strain sensors [15]. Among those, IMUs hold great promise for measuring 3D joint angles because they are lightweight, affordable, and widely available in the market [11]. An IMU commonly consists of 3-degree-of-freedom (DOF) accelerometer, gyroscope, and magnetometer. Besides the advantages mentioned above, inertial motion capture systems (IMCSs) that rely on IMUs have their own disadvantages. Firstly, the misalignment between the IMU local frame and the anatomical frame of the body segment is one of the factors that reduce the accuracy of the measured angles [16]. Secondly, because the 3D orientation of an IMU is commonly obtained by integrating the angular velocity from the gyroscope data, the error due to bias and noise can grow over time [17]. By using the data from the accelerometer and the magnetometer as the reference axes, the orientation drift can be reduced. However, for human locomotion applications, the compensation from the accelerometer becomes less effective during highly dynamic motions, in which the acceleration of the body segment is larger than the gravitational acceleration [13], [24]. On the other hand, because of the nonuniform magnetic field in most indoor environments, heading corrections based on magnetometer readings are often ineffective [18].

To address the IMU-to-segment misalignment problem, two main approaches are commonly used: anatomical calibration [19], [20] and functional calibration [21]–[24]. Compared to anatomical calibration, functional calibration provides more accurate results [21]. In [22], a novel functional calibration procedure was proposed to estimate the elbow joint angles using angular velocity vectors. Another functional calibration procedure was proposed in [23] for measuring 3D knee joint angles. The authors of [24] introduced a functional calibration method for segment orientation estimation, which was adapted for skiing tasks. In practice, however, it is difficult for the subject to exactly perform the calibrating movements required for specific joints. As an alternative, a self-calibrating method which solves the misalignment issue as a constrained weighted least squares problem in a sliding window fashion was proposed in [26]. The method was inspired by the optimization-based approach in [27]. In most of the studies summarized above, optical motion capture systems (OMCSs) provided ground truth data to validate a proposed calibration method for wearable IMCSs. Because the relative orientation between the markers of the OMCSs and the corresponding anatomical axes is not precisely known, functional calibration can improve the accuracy of both OMCSs and IMCSs [22].

Ton T. H. Duong, H. Zhang and D. Zanotto (dzanotto@stevens.edu) are with the Wearable Robotic Systems (WRS) Lab, Stevens Institute of Technology, Hoboken 07030 NJ, USA.

T. Sean Lynch is with Department of Orthopedic Surgery at Columbia University Irving Medical Center, New York 10027 NY, USA.

This work was partially supported by the US National Science Foundation under Grant IIS-1838799.

Unlike OMCSs, the accuracy of IMCSs is negatively affected by drift. This makes the relationship between IMCSs estimates and true anatomical data nonlinear and time-varying, even after functional calibration is applied. Common approaches to address this issue include sensor fusion algorithms [17]–[19] and methods based on biomechanical constraints [24]–[27]. These approaches often result in long setup time and are typically not suitable for implementation on embedded microcontrollers for out-of-the-lab applications. Notably, some approaches take advantage of the periodic nature of human locomotion to reduce the drift using Fourier-based integration and quaternion-based strap-down integration [28], [29]. These methods, however, have not been validated for measuring joint angles in walking motion.

In this paper, a novel 2-step calibration method applicable to lower-extremity IMCSs is introduced and validated in a custom-engineered device designed for the estimation of bilateral hip joint angles. The first step, functional calibration, aims at determining the orientation of the body-worn IMUs relative to the wearer's anatomical axes. In the second step, the cyclical nature of human locomotion is leveraged to reduce drift and systematic errors in the IMCS estimates. A series of linear models locked to the phase of the gait cycle approximate the complex relationship between the corrected joint angles produced in step 1 and the true anatomical angles, thus improving accuracy. The rationale behind the proposed method is twofold: (i) linear models do not require large computational power, and therefore they can be implemented in embedded controllers for lightweight wearable robotic devices; (ii) the gait phase can be reliably extracted online by applying well-known techniques [30], [31], which are commonly used to inform the high-level controllers in many existing lower-extremity wearable devices, including robotic prostheses, orthoses, and suits [32]–[34].

This paper is organized as follows. Section II describes the IMCS in detail. Section III provides the details about the methods. Section IV presents the results. Section V discusses the outcomes and presents the conclusion of the study.

II. System Description

The custom-designed IMCS proposed in this work consists of a belt module, two instrumented insoles, and a wireless data logger. As shown in Fig. 1, the belt module consists of three 9-DOF IMUs (Yost Labs Inc., OH, USA): one located on the sacrum, two located on the lateral side of each thigh and secured by Velcro straps. The IMUs are connected via serial ports to a 32-bit microcontroller (ARM Cortex-M4F, PJRC, OR, USA) which is secured inside the belt. The belt module is powered by a small 7.4V, 860mAh Li-Po battery through a 5V step-down voltage regulator. Four reflective markers are attached to a custom-built enclosing case on each IMU for validation with the OMCS. Markers placement on the sacrum IMU is based on [35]. The overall weight of the belt module including all components is approximately 400g.

The design of the instrumented insoles, named the *SportSole*, has been described in detail elsewhere [36], [37]. The *SportSole* system includes a multi-cell piezo-resistive insole

Fig. 1: Custom-made IMCS consisting of a belt module and a pair of instrumented shoes, *SportSole*.

(IEE, Luxemburg) and a 9-DOF IMU sandwiched between two layers of abrasion-resistive foam. The integrated logic, a Wi-Fi module, and a battery pack are housed inside a small enclosure that is secured to the posterolateral side of the subject's own shoes. Each insole weights less than 70g, including the on-board power and electronics.

Data are sampled at 200 Hz and 500 Hz by the belt module and by the insoles, respectively. Data are sent through Universal Datagram Protocol (UDP) using Wi-Fi (IEEE 802.11) to a data logger – a single-board computer (ODROID-C2, Hardkernel Co., GyeongGi, South Korea) which runs a Linux distribution with a real-time kernel. The same data are also streamed to a graphical user interface (GUI) running on the experimenter's laptop. The GUI allows the experimenter to control the device remotely throughout the functional calibration process and to visualize the acquired data. Accurate synchronization between the belt module and the insoles is achieved using *Broadcast Reference Time Synchronization* [39]. In this study, the *SportSole* was used only to segment the subject's hip angles, measured by the belt module, into individual strides. Indeed, the method described in the following relies on precise gait cycle segmentation. For this reason, piezo-resistive sensors embedded in the insoles were preferred over other methods (e.g., using the acceleration signals from the hip or sacrum IMUs).

III. Methods

A. Experimental Protocol

Eight healthy male adults (age: 24.7 ± 3.5 years, height: 177.8 ± 13.9 cm, weight: 72.2 ± 8.6 kg) participated in this study. The purpose of these tests was to validate the accuracy of the proposed 2-step calibration process in measuring hip

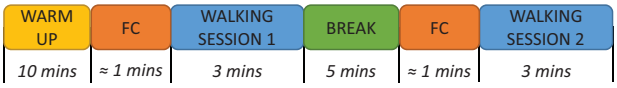

Fig. 2: Experimental Protocol (FC = Functional Calibration)

angles in walking tasks at various speeds. The protocol was approved by the Stevens Institute of Technology Institutional Review Board and all subjects gave written informed consent prior to the experimental sessions.

At the beginning of each session, the experimenter assisted the subject in donning the belt module and the insoles. The subject was then instructed to complete a 10-minute warmup session (Fig. 2) on a dual-belt treadmill instrumented with force plates (Bertec ITC-11-20L), to familiarize with the system. In this session, the subject first started walking at a random slow treadmill speed. The experimenter slowly increased the speed by 0.03 m/s steps until the subject reached a comfortable walking speed (CWS). The process was repeated two additional times with the speed starting from 0.42m/s above and below the first determined comfortable speed, respectively [38]. The final CWS was the average of all three trials. Throughout this session, the treadmill speed was blinded to the subject. Next, subjects were instructed to perform two 3-minute walking bouts on the treadmill: one at 85% and one at 115% of their CWS. The order of the slow/fast bouts was randomized across the subjects. Before each walking bout, functional calibration was performed to align the IMUs to the body segments, as described in the following section. There was a 5-minute break after each test and the subject did not remove the IMCS until the end of the experimental session. During each test, the positions of the reflective marker clusters were captured by an 8-camera OMCS (VICON Vero 2.2, Oxford, UK), which was used as the reference system. A custom-made wireless board working at 500 Hz was used to synchronize the OMCS to the IMCS using a cluster of infrared LEDs [39].

B. Functional Calibration

In order to align the local frames of the IMUs and the markers clusters to the anatomical axes of the body segments, subjects were asked to perform the sequence of movements shown in Tab. I. The coordinate systems of the pelvis and two femurs were defined based on ISB recommendations [40].

For each movement, subjects were asked to perform 3 repetitions within 3 seconds. For the thigh abduction movements, subjects were asked to land their feet back to the initial position after performing each repetition. The angular velocity vectors of the IMU which corresponded to the segment being calibrated were recorded in matrix M . The covariance matrix C was computed for matrix M and eigendecomposition was applied on C to determine the principal axes of the calibration movement. The normalized eigenvector $\vec{v}$ which corresponds to the largest eigenvalue λ_{max} of C was chosen to be the principle rotating axis of the calibrating movement [22].

TABLE I: Functional calibration movements

Segments	*Movement*	*Calibrated Axis*
Pelvis	Trunk flexion/extension	Pelvis z-axis
	Trunk rotation right/left	Pelvis y-axis
Thighs	Squat with knees in parallel	Thighs z-axes
	Right thigh abduction	Right thigh x-axis
	Left thigh abduction	Left thigh x-axis

As shown in Table I, two types of calibration movements were performed for each segment, yielding the orientation of two anatomical axes per each segment, relative to the IMU local frame. The third axis was then computed from the cross product of these two, and the IMU-to-segment transformation matrix $R_{IMU}^{segment}$ was constructed from these three orthogonal axes. For instance, the transformation matrix to align the IMU on the sacrum to the pelvis segment was determined as follows.

$$\vec{i}_{Pelvis} = \vec{j}_{Pelvis}^{temp} \times \vec{k}_{Pelvis} \tag{1}$$

$$\vec{j}_{Pelvis} = \vec{k}_{Pelvis} \times \vec{i}_{Pelvis} \tag{2}$$

$$R_{IMU}^{Pelvis} = \begin{bmatrix} \vec{i}_{Pelvis} & \vec{j}_{Pelvis} & \vec{k}_{Pelvis} \end{bmatrix} \tag{3}$$

where $\vec{j}_{Pelvis}^{temp}$ is the temporary y-axis obtained from the trunk rotation movement. This axis was then corrected using (2) to maintain the orthonormal property of the unit vectors in a transformation matrix.

After the segments were calibrated, subjects were asked to stand still in the upright neutral position for 5 seconds in order to obtain the average gravity vectors $\vec{g}$ in the IMU local frames. In this pose, we assumed that all vectors $\vec{k}_{segment}$ pointed to the right of the body [40]. Thus, the IMU-to-global transformation matrix R_{IMU}^{glob} for each IMU was obtained as follows:

$$\vec{j}_{glob} = -\vec{g} \tag{4}$$

$$\vec{i}_{glob} = \vec{j}_{glob} \times \vec{k}_{segment} \tag{5}$$

$$\vec{k}_{glob} = \vec{i}_{glob} \times \vec{j}_{glob} \tag{6}$$

$$R_{IMU}^{glob} = \begin{bmatrix} \vec{i}_{glob} & \vec{j}_{glob} & \vec{k}_{glob} \end{bmatrix} \tag{7}$$

Knowing the IMU-to-global and IMU-to-segment transformations for each segment, two rotational matrices describing the relative orientations between the left/right thighs and the pelvis could be determined, from which the left and right hip angles (flexion/extension, abduction/adduction) were extracted [41]. Although hip internal/external rotation, in principle, can be computed using the same method, transverse plane motion was not considered in this study, which focuses on measuring the anterior/posterior and medio/lateral hip kinematics in walking motion, i.e., the hip DOF that are usually actuated in lower-extremity exoskeletons [42].

For validation purposes, the functional calibration procedure described above was applied also to OMCS marker clusters to obtain ground-truth estimates.

C. Phase-locked Linear Regression Models

In the second step of the calibration procedure, regression models were applied to reduce drift and other systematic errors in the raw estimates of the hip angles determined in step 1. These phase-locked models take advantage of the cyclical nature of human locomotion. In addition to the raw hip angles, a set of scalar covariates are fed as inputs to the models. Two calibration approaches, *subject-specific* and *generic*, are proposed to train the models. Once trained, the models can run on the IMCS' embedded logic (assuming that an on-line estimate of the gait phase is available, e.g., using phase oscillators [30], [31]) in the unconstrained environment, without the need for the OMCS.

To train the regression models, hip flexion/extension (FE) and abduction/adduction (AA) obtained with the IMCS and OMCS were first segmented into gait cycles (using insoles data and force plates data, respectively), then time-normalized into a set of $N = 101$ equally spaced data points (i.e., 0-100% of the gait cycle, GC). Stride time (ST), root mean square (RMS) of the thigh angular velocity over the GC (ω_{RMS}), and elapsed time (ET) were regarded as candidate covariates for all the models.

Further, data from slow and fast walking bouts were pooled prior to calibration, with the goal of deriving models that are robust within a broad range of walking speeds.

1) Subject-specific Calibration: This calibration method generates a set of regression coefficients that are optimal, in the least squares (LS) sense, for a particular subject. This approach yields high accuracy at the expense of longer setup time, since reference data must be measured from the subject prior to data collection. On the other hand, after calibration, the subject's hip angles can be measured in the unconstrained environment.

N independent linear regression models were generated in the following form:

$$Y^O_{tr,i} \sim \hat{Y}^I_{tr,i} + x_{1,i} + x_{2,i} + \ldots + x_{r,i}, i \in [1, N] \qquad (8)$$

where Y represents the generic hip angle (FE, AA) measured with either the OMCS (superscript O) or with the IMCS (superscript I), the index i refers to the percentage of the GC, x_* are a set of r covariates, and the subscript tr indicates the training dataset. These models yielded a set of $(r + 2)$ optimal regression coefficients $\bar{\beta}_{j,i}$ from which the estimate of Y can be computed as:

$$\hat{Y}^O_i = \bar{\beta}_{0,i} + \bar{\beta}_{1,i} Y^I_i + \sum_{k=1}^{r} \bar{\beta}_{k+1,i} x_k, i \in [1, N] \qquad (9)$$

10-fold cross validation [43] was used to validate these models, and the final regression coefficients were obtained by averaging across the 10 folds. Further, the optimal set of regressors for each hip angle was extracted among the group of candidate regressors by checking all possible combinations of regressors for all subjects through cross-validation, and by selecting the model yielding the least RMS error (RMSE) across all subjects. For the two hip angles, the optimal set of regressors was found to coincide with the full set.

2) Generic Calibration: This approach represents the common application of the IMCS, when collecting reference data is either unfeasible or unpractical, thereby the calibration model must account for inter-subject variability. The generic models are similar to (8) and (9), except that an additional candidate regressor, subject's body mass index, was considered. These models were trained and validated using *leave-one-out crossvalidation* [44]. Similar to the subject-specific calibration, exhaustive search was adopted to identify the best subset of regressors, i.e., the one yielding the least RMSE for each angle. This optimization indicated the corresponding hip angle estimated from step 1 as well as ET as the optimal set of regressors. ET is regarded as the regressor that most account for drift correction.

D. Data Analysis

For each subject, the mean absolute error (MAE), the RMSE, the SD of the error and the coefficient of determination (R^2) were computed for each type of calibration and for each hip angle. For both angles, group averages of the MAE were compared through paired t-tests, in order to assess significant ($\alpha = 0.05$) differences among the types of calibration.

IV. Results

A total of 2124 gait cycles was collected by the wearable system and by the reference system. Depending on subject's walking speed, which ranged from 0.86 m/s to 1.73 m/s (1.12 ± 0.15 m/s), the number of gait cycles per subject varied from 225 to 300 (276.2 ± 24.14). Fig. 3 illustrates the effect of the type of calibration on the estimated hip angle trajectories for a representative subject. Fig. 4 shows the MAE of each hip angle, under the three calibration modes considered. Tab. 2 shows the average error metrics across all subjects for each calibration method.

For the FE angles, both the *subject-specific* and the *generic* models were effective in significantly reducing the residual systematic errors after functional calibration was applied ($p<.001$ and $p<.05$, respectively) even though, as expected, the former method resulted in higher accuracy ($p<.01$).

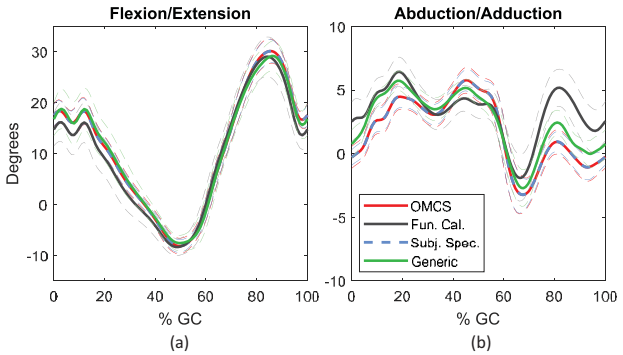

Fig. 3: Average hip joint trajectories for a representative subject. Bounded areas indicate +/- 1SD.

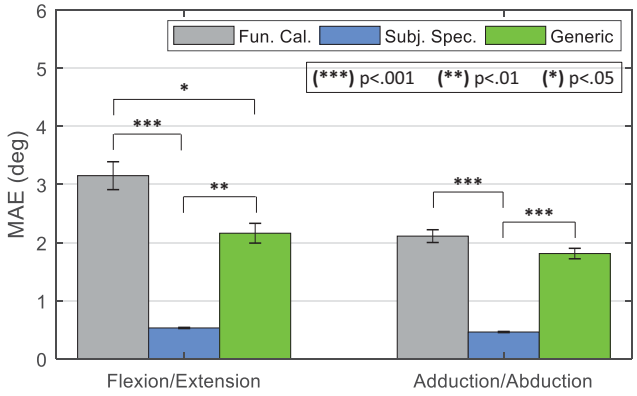

Fig. 4: Group averages of the MAE for the hip angles, separated by type of calibration. Error bars indicate +/-1SE.

A similar trend was found for the AA angle, with the MAE being significantly reduced for the *subject-specific* calibration compared to both the functional calibration ($p<.001$) and the *generic* calibration ($p<.001$). However, the *generic* calibration did not reduce the MAE significantly, relative to the functional calibration.

V. Discussion and Conclusion

This paper presented a simple and yet effective method to improve the accuracy of inertial motion capture systems, which leverages the periodic nature of human locomotion by using phase-locked regression models. The approach was validated on a custom-engineered IMCS designed to track bilateral hip angles. The proposed 2-step calibration method is computationally simple and therefore suitable for real-time embedded systems. Even though the method was tested on hip angles, in principle it can be applied to other joints of the lower-limb (i.e., knee and ankle), which are less complex than the hip joint. Because many existing lower-extremity robotic exoskeletons and prostheses feature embedded estimators of the gait phase [33], [34], the proposed approach has the potential to be readily deployed in those systems.

By adopting the *subject-specific* models, the accuracy of the IMCS in estimating the hip angles was significantly improved. Compared to the results reported by the authors of [18], the proposed approach yielded lower average RMSE for both hip angles. The IMU-to-segment alignment procedure presented in that study required an OMCS, which makes it impractical for out-of-the-lab applications. Conversely, in the proposed approach, functional calibration was applied on-line on embedded logic before data collection, without the need for a reference system. Additionally, all *subject-specific* models yielded accurate results within a broad range of walking speeds (i.e. within +/-15% of subject's CWS), whereas the effect of varying speed was not assessed by previous works.

Furthermore, the *subject-specific* method proposed in this paper was effective in correcting drift by encoding the effects of error build-up at the beginning and ending of the gait cycle in the phase-locked models [29]. Although different drift correction methods which exploit the cyclical nature of human gait were proposed in the past [28], [29], these methods were not validated for measuring joint angles in walking motion. Other approaches presented in [17], [24], [25], [27]–[29] can also reduce the errors due to drift by relying on more complex correction techniques (i.e., sensors fusion and biomechanical constraints). However, differences in terms of experimental protocol and type of investigated motor tasks make any direct comparison with the proposed approach impossible.

Although the *generic* calibration proved to be effective in further reducing systematic errors for the hip flexion/extension angle, no significant improvement compared to the functional calibration data was found for the abduction/adduction angle. This limitation might have resulted from the high inter-subject variability in the data. Errors in the functional calibration movements could also have caused subject-specific orientation offsets that are difficult to compensate with a generic model. This issue was also described in other studies [18], [24].

In general, both the *subject-specific* and the *generic* models improved the goodness of fit (R^2) of the data obtained with functional calibration. This suggests that phase-locked models can effectively correct the maximum/minimum range of motion error [18], which commonly occurs at specific phases of the gait cycle.

Future work will include improving the robustness of the *generic* models against inter-subject variability, e.g., by introducing learning-based regression models, which have better expressive power than linear models. Moreover, a larger sample will be collected to train the *generic* calibration models, and the test-retest reliability of *subject-specific* models will be studied. The performance of these models in highly dynamic tasks, such as running and jumping, will also be evaluated.

TABLE II:
Average RMSE, MAE, Error SD AND R^2
(All angles are in degree)

Angle		RMSE	MAE	STD	R^2
FE	Fun. Cal.	3.68	3.15	2.35	0.96
	Subj. Spec.	0.68	0.53	0.67	0.99
	Generic	2.58	2.18	1.80	0.98
AA	Fun. Cal.	2.51	2.11	1.92	0.83
	Subj. Spec.	0.59	0.46	0.59	0.98
	Generic	2.21	1.82	1.74	0.84

References

[1] B. S. Rupal, S. Rafique, A. Singla, E. Singla, M. Isaksson, G. S. Virk, "Lower-limb exoskeleton: Research trends and regulatory guidelines in medical and non-medical applications," International Journal of Advanced Robotic Systems, pp: 1-27, 2017.

[2] H. Herr, "Exoskeletons and orthoses: classification, design challenges and future directions," Journal of NeuroEngineering and Rehabilitation, 6:21, 2009.

[3] A. M. Dollar, H. Herr, "Lower extremity exoskeletons and active orthoses: challenges and state-of-the-art," IEEE Transaction on Robotics, Vol. 24, No. 1, 2008.

[4] H. Kawamoto, Y. Sankai, "Power assist system HAL-3 for gait disorder person," Proceedings of the 8th International Conference on Computers Helping People with Special Needs, pp: 196-203, 2002.

[5] D. Zanotto, P. Stegall, S. K. Agrawal, "ALEX III: A novel robotic platform with 12 DOFs for human gait training," IEEE International Conference on Robotics and Automation, 2013.

[6] D. Zanotto, Y. Akiyama, P. Stegall, S. K. Agrawal, "Knee joint misalignment in exoskeletons for the lower extremities: Effects on user's gait," IEEE Transactions on Robotics, 31 (4), pp: 978-987, 2015.

[7] D. Zanotto, T. Lenzi, P. Stegall, S. K. Agrawal, "Improving transparency of powered exoskeletons using force/torque sensors on the supporting cuffs," IEEE International Conference on Rehabilitation Robotics (ICORR), 2013.

[8] A. T. Asbeck, R. J. Dyer, A. F. Larusson, C. J. Walsh, "Biologically-inspired Soft Exosuit," IEEE International Conference on Rehabilitation Robotics, 2013.

[9] M. Wehner, B. Quinlivan, P. M. Aubin, E. Martinez-Villalpando, M. Baumann, L. Stirling, K. Holt, R. Wood, C. Walsh, "A lightweight soft exosuit for gait assistance," IEEE International Conference on Robotics and Automation, 2013.

[10] Y. Ding, I. Galiana, A. Asbeck, B. Quinlivan, S. M. M. D. Rossi, C. Walsh, "Multi-joint actuation platform for lower extremity soft exosuit," IEEE International Conference on Robotics and Automation, 2014.

[11] D. T. Fong, Y. Chan, "The use of wearable inertial motion sensors in human lower limb biomechanics studies: A systematic review," Sensors, 10, pp:11556-11565, 2010.

[12] L. C. Benson, C. A. Clermont, E. Bosnjak, R. Ferber, "The use of wearable devices for walking and running gait analysis outside of the lab: A systematic review," Gait & Posture, 63, pp: 124-138, 2018.

[13] V. Camomilla, E. Bergamini, S. Fantozzi, G. Vannozzi. "Trends supporting the in-field use of wearable inertial sensors for sport performance evaluation: A systematic overview," Sensors, 18, 2018.

[14] P. T. Gibbs, H. H. Asada, "Wearable conductive fiber sensors for multi-axis human joint angle measurements," Journal of NeuroEngineering and Rehabilitation, 2005.

[15] Y. Menguc, Y. Park, E. Martinez-Villalpando, P. Aubin, M. Zisook, L. Stirling, R. J. Wood, C. J. Walsh, "Soft wearable motion sensing suit for lower limb biomechanics measurements," IEEE International Conference on Robotics and Automation, pp: 5309-5316, 2013.

[16] L. S. Vargas-Valencia, A. Elias, E. Rocon, T. Bastos-Filho, A. Frizera, "An IMU-to-body alignment method applied to human gait analysis," Sensors, 2016.

[17] E. Bergamini, G. Ligorio, A. Summa, G. Vannozzi, A. Cappozzo, A. M. Sabatini, "Estimating orientation using magnetic and inertial sensors and different sensor fusion approaches: Accuracy assessment in manual and locomotion tasks," Sensors, 2014.

[18] W. Teufl, M. Miezal, B. Taetz, M. Frohlich, G. Blesser, "Validity, test-retest reliability and long-term stability of magnetometer free inertial sensor based 3D joint kinematics," Sensors, 2018.

[19] M. Miezal, B. Taetz, G. Bleser, "On inertial body tracking in the presence of model calibration errors," Sensors, 2016.

[20] E. Palermo, S. Rossi, F. Marini, F. Patane, P. Cappa, "Experimental evaluation of accuracy and repeatability of a novel body-to-sensor calibration procedure for inertial sensor-based gait analysis," Measurement, 52, pp: 145-155 2014.

[21] W. De Vries, H. Veeger, A. Cutti, C. Baten, and F. Van der Helm, "Functionally interpretable local coordinate systems for the upper extremity using inertial & magnetic measurement systems," Journal of Biomechanics, 43 (10), pp. 1983–1988, 2010.

[22] G. Ligorio, D. Zanotto, A. M. Sabatini, S. K. Agrawal, "A novel functional calibration method for real-time elbow joint angles estimation with magnetic-inertial sensors," Journal of Biomechanics, 54, pp: 106-110, 2017.

[23] J. Favre, R. Aissaoui, B. M. Jolles, J. A. de Guise, K. Aminian, "Functional calibration procedure for 3D knee joint angle description using inertial sensors," Journal of Biomechanics, 42, pp: 2330-2335, 2009.

[24] B. Fasel, J. Sporri, P. Schutz, S. Lorenzetti, K. Aminian, "Validation of functional calibration and strap-down drift correction for computing 3D joint angles of knee, hip, and trunk in alpine skiing," PLoS ONE, 12 (7), 2017, e0181446.

[25] B. Fasel, J. Sporri, J. Chardonnens, J. Kroll, E. Muller, K. Aminian, "Joint inertial sensor orientation drift reduction for highly dynamic movements," IEEE Journal of Biomedical and Health Informatics, Vol. 22, No. 1, 2018.

[26] B. Taetz, G. Bleser, M. Miezal, "Towards self-calibrating inertial body motion capture," International Conference on Information Fusion, 2016.

[27] M. Kok, J. D. Hol, T. B. Schon, "An optimization-based approach to human body motion capture using inertial sensors," The International Federation of Automatic Control, 2014.

[28] A. M. Sabatini, G. Ligorio, A. Mannini, "Fourier-based integration of quasi-periodic gait accelerations for drift-Free displacement estimation using inertial sensors," BioMedical Engineering OnLine, 2015.

[29] A. M. Sabatini, "Quaternion-based strap-down integration method for application of inertial sensing to gait analysis," Medical and Biological Engineering and Computing, 43, 2005.

[30] L. Righetti, J. Buchli, A. J. Ijspeert, "Adaptive Frequency Oscillators and Applications," The Open Cybernetics and Systemics Journal, 3, pp: 64-69, 2009.

[31] T. Petric, A. Gams, A. J. Ijspeert, L. Zlajpah, "On-line frequency adaptation and movement imitation for rhythmic robotic tasks," The International Journal of Robotics Research, 30 (14), pp: 1775-1788, 2011.

[32] T. Yan, M. Cempini, C. M. Oddo, N. Vitiello, "Review of assistive strategies in powered lower-limb orthoses and exoskeletons," Robotics and Autonomous Systems, 64, pp:120-136, 2015.

[33] R. Jimenez-Fabian, O. Verlinden, "Review of control algorithms for robotic ankle systems in lower-limb orthoses, prostheses, and exoskeletons," Medical Engineering & Physics, 34, pp: 397-404, 2012.

[34] D. Zanotto, P. Stegall, S. K. Agrawal, "Adaptive assist-as-needed controller to improve gait symmetry in robot-assisted gait training." IEEE International Conference in Robotics and Automation, pp: 724-729, 2014.

[35] M. Borhani, A. H. McGregor, A. M. J. Bull, "An alternative marker set for the pelvis is more repeatable than the standard pelvic marker set." Gait & Posture, 38, 2013.

[36] H. Zhang, D. Zanotto, S. K. Agrawal, "Estimating CoP trajectories and kinemtic gait parameters in walking and running using instrumented insoles," IEEE Robotics and Automation Letters, Vol. 2, No. 4, pp: 2159-2165, 2017.

[37] H. Zhang, M. Tay, Z. M. Suar, M. Kurt, D. Zanotto. "Regression Models for Estimating Kinematic Gait Parameters with Instrumented Footwear," IEEE International Conference on Biomedical Robotics and Biomechatronics, 2018.

[38] U. Dal, T. Erdogan, B. Resitoglu, H. Beydagi, "Determination of preferred walking speed on treadmill may lead to high oxygen cost on treadmill walking," Gait & Posture, 31 (3), pp: 366-369, 2010.

[39] J. Elson, L. Girod, D. Estrin. "Fine-grained network time synchronization using reference broadcast." ACM SIGOPS Operating Systems Design and Implementation, Vol. 36, Iss. SI, pp: 147-163, 2002.

[40] G. Wu, S. Siegler, P. Allard, C. Kirtley, A. Leardini, D. Rosenbaum, et at. "ISB recommendation on definitions of joint coordinate system of various joints for the reporting of human joint motion - Part I: ankle, hip, and spine," Journal of Biomechanics, 35 (4), pp: 543-548, 2002.

[41] R. V. Vitali, S. M. Cain, R. S. McGinnis, A. M. Zaferiou, L. V. Ojeda, S. P. Davidson, N. C. Perkins. "Method for Estimating Three-Dimensional Knee Rotations Using Two Inertial Measurement Units: Validation with a Coordinate Measurement Machine," Sensors, 2017.

[42] S. Vitekkova, P. Kutilek, M. Jirina, "Wearable lower limb robotics: A review," Biocybernetics and Biomedical Engineering, 33, 96-105, 2013.

[43] R. Kohavi, "A study of cross-validation and bootstrap for accuracy estimation and model selection," International Joint Conference on Artificial Intelligent, 1995.

[44] R. O. Duda, P. E. Hart, D. G. Stork, "Pattern Classification," Wiley, 2012.